Journal of Nanoscience & Technology
Volume 1| Issue 1

Research Article Open Access

Vibration of Single-Walled Carbon Nanotube Resting on Elastic Foundation with Magnetic and Thermal Effects under the Influence of Casimir Force

EH Abubakar[1], MG Sobamowo[2], MO Sadiq[1], AA Yinusa[2*]

[1]Civil and Environmental Engineering Department, University of Lagos, Nigeria
[2]Mechanical Engineering Department, University of Lagos, Nigeria

[*]**Corresponding Author:** AA Yinusa, Mechanical Engineering Department, University of Lagos, Nigeria, Tel.: 08023155984, E-mail: aayinusa@unilag.edu.ng

Citation: EH Abubakar, MG Sobamowo, MO Sadiq, AA Yinusa (2023) Vibration of Single-walled Carbon Nanotube Resting on Elastic Foundation with Magnetic and Thermal Effects under the Influence of Casimir Force, J Nanosci Technol 1(1): 103

Received Date: November 12, 2023 **Accepted Date:** December 12, 2023 **Published Date:** December 16, 2023

Abstract

Nonlinear vibration analysis of dynamic response of carbon nanotube has created noble attention globally because of their properties and applications in tomorrow's society. In this study, vibration of single-walled carbon nanotubes resting on elastic foundation with magnetic and thermal effects under the influence of Casimir force is presented. The beam is model on the basis of Eringen's nonlocal elasticity theory and Euler-Bernoulli beam theory which are used to derive the governing nonlinear partial differential equation of motions. The governing nonlinear partial differential equation is decomposed after introducing dimensionless parameters into ordinary differential equation using Galerkin decomposition method and the resulting equation is solve analytically using Homotropy Perturbation Method. Simulations reveal that, effects of parameters on dynamic responses which are studied and discussed in full details.

Keywords: Single-walled Carbon Nanotubes; Magnetic, Thermal; Homotopy Perturbation Method, Elastic Foundation and Casimir Force.

Introduction

The dynamic response analysis of nanotube (CNTs) has created attention owing to their excellent potential properties and usage in fields of nanoscience, mechanical and electrical engineering since the evolution of the tiny materials decades ago. Consequently, research into nonlinear vibrational and unreliability analysis of fluid conveying double walled carbon nanotubes on elastic spring foundation has been presented [20]. Furthermore, non-local elastic and Euler-Bernoulli beams theories were used in modeling the nonlinear system. Another research work investigated stability of pinned-pinned supports double-walled carbon nanotubes conveying flow in its inner tube which considered vdW interactions between the adjacent tube layers [6]. Euler elastic beam model was use to studied the dynamic stability response of the nonlinear system under investigation. An investigation into the flexural nonlinear vibration analysis of curved SWCNTs embedded in spring foundation using non-local Euler-Bernoulli beams model has been carried out [11]. A research work employed analytical method to investigate surface effects on vibration and instabilities of fluid conveying tubes fixed in viscoelastic foundation [19]. Investigation has been carried out on the stability of zigzag, chiral, and armchair single-walled carbon nanotubes resting on Winkler elastic medium under both lower and higher temperature environment [16]. A presentation has been published on the nonlinear vibration behaviour of single-walled carbon nanotube [18]. The SWCNT is modeled as a pinned-pinned supports beam fixed into the elastic foundation and Euler Bernoulli beam theory was used to developed the nonlinear equations of motions. The resulting nonlinear governing equation of motions was solved using homotopic perturbation method (HPM) and elliptical functions. Moreso, obtained results of elliptical functions were compared with those obtained with HPM analysis and effects of elastic parameters, axial force, flow velocity as well as variations between linear and nonlinear frequencies were fully investigated. Vibrational analysis of single-walled carbon nanotube fixed in polymer matrices and aroused by vdW force using elasticity beam model has been studied [7]. The interfacial van der Waals force was described by non-linear functions in term of deflection of carbon nanotubes using distinct ends supports and harmonical balance method. This resulting system was found to be sensitively to boundary conditions, tube diameter and lengths of the fixed CNTs. Furthermore, the influences of axial load on the vibration behaviors of CNTs during post-buckling were fully discussed. A nonlinear model for free vibrational analysis of SWCNTs conveying fluid has been put forward [2]. For the analysis, the study employed numerical simulation via von-Kármán geometric nonlinearity and Eringen non-local elasticity theories. Furthermore, the single-walled carbon nanotube was modelled in form of nanobeams where effect of transverse shear deformation and rotary inertia are considered within the framework of Timoshenko beams theory. Again, nonlinear governing equation of motion and end supports conditions were modelled with Hamilton's principle and solved by analytically. The critical flow velocity, frequency amplitude relationship with flutter and divergence instability and associated time responses were obtained using the above methodology. An investigation into the stability of periodical heterogeneous carbon nanotubes conveying fluid has been performed and reported [5]. The study used Euler-Bernoulli beam's theory to derived the nonlinear governing equation of motions of the system. Afterwards, dynamical stiffness method (DSM) analysis was employed to determine the stability and critical fluid velocity of the hetero carbon nanotubes. In conclusion, the parametric studies performed using the results, reveal that with proper selection of parameters such as length-ratio, stability of constructed carbon nanotubes can be enhanced. The phenomenon of static and buckled analyses of carbon nanotube with developed non-local continuum model and small-scale effects were explicitly derive for bending deformations of carbon nanotube subjected to flexural loading conditions [12]. A detailed discussions on several derivative of flexural term for the carbon nanotube from existing experimental works were provided. An exploration into the effects of non-local elasticity theory on electromechanical behaviors of SWCNTs under electrostatic actuation has been carried out [8]. Similarly, a study on the dynamic stability of CNTs embedded in elastic matrix under the influence of time dependent axially loaded system has been performed [1]. The effects of longitudinally induced magnetic fields on transverse vibration of SWCNTs conveying fluid under non-local elasticity theory and non-local beam model have been scrutinized [9]. Another study investigated chaotical behavior of single-walled carbon nanotube with linearly and nonlinearly damping system using Hamilton's principle and Galerkin's method of analysis [17]. In another research, the vibration instability characteristic of double walled carbon nanotubes under several configurations has been studies with hybrid approaches [13]. The studied depict that curving instability takes place through formation of single-kink in mid-point of DWCNTs or double-kink, place symmetrically at mid-point, depending on both the length and the diameter of the CNTs under investigation. Variational principles have been employed to analyze the stability of multi-walled carbon nanotube (MWCNTs) with different mechanical loads based on non-local elasticity of Donnell's shell [10]. The nonlinear transient behaviors of the carbon nanotube, fiber and polymer composites of spheric shells contained in central cutout of the system have been explored [14]. The multi-scale analysis was used to determine the nanotube's weight-ratios, thickness-radius-ratios, thickness length-ratios of nanotube and cutout sizes respectively. Report has been made on how SWCNT revolutionized world of nanotechnology with their exceptionally proprieties which made them to be core to several application in various field of engineering and nanoengineering. Moreso, several studies have been conducted to investigated these proprieties since their discoveries decades ago. Again, free vibrational analysis of single walled carbon nanotubes was studied in elasticity environments based on Eringen non-local theory of elastic and was solved by differential quadrature method (DQM) [3]. The vibration analysis of single-walled carbon nanotubes (SWCNTs) with incorporated longitudinally magnetic fields have been studied using Euler-Bernoulli beam and Eringen's nonlocal elastic theories [15]. Recently, a research work analyzed the dynamic response of single wall carbon nanotube partially fixed with elastic foundation via Euler Bernoulli beam and non-local elasticity theories. An analytical technique was adopted to solved the governing partial differential equation of motion of the nanotube structures. Then, the influences of temperature, non-local parameter and coefficients of elasticity of foundation were analyzed and discussed extensively during parametric studied. Finally, the obtained results show that, temperature effects, non-local parameter and coefficients of elasticity foundation are important on the natural frequency of carbon nanotubes [4]. Other relevant studies on the modelling and analysis of nanotubes have been presented [21-26] The potential applications of nanotubes have been elaborated. However, to the best of our knowledge, previous studies have neglected analytical approach towards investigating the vibration of nanotubes with thermal-magnetic effects and Casimir force acting simultaneously. Motivated by the aforementioned gap, this present study presents vibration of SWCNT resting on elastic foundation with magnetic and thermal effects under the influence of Casimir force. The results of this study will contribute immensely to the advancements in nanotechnology, mechanical engineering and other relevant fields

Formulation of Model

The formulation of nonlinear governing equation of motion under consideration of single walled carbon nanotube resting on Winkler-type elastic medium is presented in Eq. (1). The problem was modelled on the basis of Eringen's nonlocal elasticity theory couple with Euler Bernoulli Beams theory. The longitudinal magnetic field of Maxwell's equation is also adopted.

$$\mathrm{EI}\frac{\partial^4 w}{\partial x^4}+m\frac{\partial^2 w}{\partial t^2}-\eta \mathrm{H}_x^2\mathrm{A}\frac{\partial^2 w}{\partial x^2}+\mathrm{K}w-(e_0 a)^2\frac{\partial^2}{\partial x^2}\left(m\frac{\partial^2 w}{\partial t^2}-\eta \mathrm{H}_x^2\mathrm{A}\frac{\partial^2 w}{\partial x^2}+\mathrm{K}w\right)=0 \quad (1)$$

The Winkler foundation usually represented as $\mathrm{K}w$ can denotes for both linear Winkler and nonlinear Winkler type elastic foundation. That is, $\mathrm{K}w = k_1 w + k_3 w^3$, where $k_1 w$ is the linear Winkler and $k_3 w^3$ is the nonlinear Winkler type. Substituting into equation (1) gives:

$$\mathrm{EI}\frac{\partial^4 w}{\partial x^4}+m\frac{\partial^2 w}{\partial t^2}-\eta \mathrm{H}_x^2\mathrm{A}\frac{\partial^2 w}{\partial x^2}+k_1 w+k_3 w^3-(e_0 a)^2\frac{\partial^2}{\partial x^2}\left(m\frac{\partial^2 w}{\partial t^2}-\eta \mathrm{H}_x^2\mathrm{A}\frac{\partial^2 w}{\partial x^2}+k_1 w+k_3 w^3\right)=0 \quad (2)$$

Also, Pasternak type foundation is acting on the system as $k_p\frac{\partial^2 w}{\partial x^2}$ where, this is the change in thermal, $\mathrm{EA}\alpha\mathrm{T}\frac{\partial^2 w}{\partial x^2}$ and the system is subjected to Casimir force, F_C. Substituting them into equation (2) yield;

$$\begin{gathered}\mathrm{EI}\frac{\partial^4 w}{\partial x^4}+m\frac{\partial^2 w}{\partial t^2}-\eta \mathrm{H}_x^2\mathrm{A}\frac{\partial^2 w}{\partial x^2}+k_1 w+k_3 w^3-\mathrm{EA}\alpha\mathrm{T}\frac{\partial^2 w}{\partial x^2}-k_p\frac{\partial^2 w}{\partial x^2}-\\(e_0 a)^2\frac{\partial^2}{\partial x^2}\left(m\frac{\partial^2 w}{\partial t^2}-\eta \mathrm{H}_x^2\mathrm{A}\frac{\partial^2 w}{\partial x^2}+k_1 w+k_3 w^3-\mathrm{EA}\alpha\mathrm{T}\frac{\partial^2 w}{\partial x^2}-k_p\frac{\partial^2 w}{\partial x^2}\right)=F_C+(e_0 a)^2\frac{\partial^2 w}{\partial x^2}F_C\end{gathered} \quad (3)$$

Substituting Casimir force, $F_C = \dfrac{\pi^3 \overline{h} c b}{240(d-w)^4}$, into equation (3) becomes;

Substituting Casimir force, $F_C = \dfrac{\pi^3 \bar{h} cb}{240(d-w)^4}$, into equation (3) becomes;

$$\begin{aligned} &\mathrm{EI}\frac{\partial^4 w}{\partial x^4} + m\frac{\partial^2 w}{\partial t^2} + k_1 w + k_3 w^3 - \left(\eta \mathrm{H}_x^2 \mathrm{A} + \mathrm{EA}\alpha\mathrm{T} - k_p\right)\frac{\partial^2 w}{\partial x^2} - \\ &\left(e_0 a\right)^2 \left(m\frac{\partial^4 w}{\partial x^2 \partial t^2} - \eta \mathrm{H}_x^2 \mathrm{A}\frac{\partial^4 w}{\partial x^4} + k_1 w\frac{\partial^2 w}{\partial x^2} + k_3 w^2 \frac{\partial^2 w}{\partial x^2} - \mathrm{EA}\alpha\mathrm{T}\frac{\partial^4 w}{\partial x^4} - k_p \frac{\partial^4 w}{\partial x^4} \right) = \\ &\frac{\pi^3 \bar{h} cb}{240(d-w)^4} + \left(e_0 a\right)^2 \frac{\partial^2 w}{\partial x^2}\left(\frac{\pi^3 \bar{h} cb}{240(d-w)^4} \right) \end{aligned} \tag{4}$$

Solving right side of equation (4) becomes;

$$\begin{aligned} &\mathrm{EI}\frac{\partial^4 w}{\partial x^4} + m\frac{\partial^2 w}{\partial t^2} + k_1 w + k_3 w^3 - \left(\eta \mathrm{H}_x^2 \mathrm{A} + \mathrm{EA}\alpha\mathrm{T} - k_p\right)\frac{\partial^2 w}{\partial x^2} - \\ &\left(e_0 a\right)^2 \left(m\frac{\partial^4 w}{\partial x^2 \partial t^2} - \eta \mathrm{H}_x^2 \mathrm{A}\frac{\partial^4 w}{\partial x^4} + k_1 w\frac{\partial^2 w}{\partial x^2} + k_3 w^2 \frac{\partial^2 w}{\partial x^2} - \mathrm{EA}\alpha\mathrm{T}\frac{\partial^4 w}{\partial x^4} - k_p \frac{\partial^4 w}{\partial x^4} \right) = \\ &\frac{\varepsilon_4}{(1-W)^4} + \left(e_0 a\right)^2 \frac{\varepsilon_6}{(1-W)^6} \end{aligned} \tag{5}$$

By series expansion of righthand side of equation (5) becomes;

$$\frac{\varepsilon_4}{(1-W)^4} = \varepsilon_4\left(1 + 4W + 10W^2 + 20W^3 + 35W^4 + 56W^5 + 84W^6 + 0\left(W^7\right)\right) \tag{6}$$

$$\frac{\varepsilon_6}{(1-W)^6} = \varepsilon_6\left(1 + 6W + 21W^2 + 56W^3 + 126W^4 + 252W^5 + 462W^6 + 0\left(W^7\right)\right) \tag{7}$$

Substituting equation (6) and (7) into equation (5) yield;

$$\begin{aligned} &\mathrm{EI}\frac{\partial^4 w}{\partial x^4} + m\frac{\partial^2 w}{\partial t^2} + k_1 w + k_3 w^3 - \left(\eta \mathrm{H}_x^2 \mathrm{A} + \mathrm{EA}\alpha\mathrm{T} - k_p\right)\frac{\partial^2 w}{\partial x^2} - \\ &\left(e_0 a\right)^2 \left(m\frac{\partial^4 w}{\partial x^2 \partial t^2} - \eta \mathrm{H}_x^2 \mathrm{A}\frac{\partial^4 w}{\partial x^4} + k_1 w\frac{\partial^2 w}{\partial x^2} + k_3 w^2 \frac{\partial^2 w}{\partial x^2} - \mathrm{EA}\alpha\mathrm{T}\frac{\partial^4 w}{\partial x^4} - k_p \frac{\partial^4 w}{\partial x^4} \right) = \\ &\left(\begin{aligned} &\varepsilon_4\left(1 + 4W + 10W^2 + 20W^3 + 35W^4 + 56W^5 + 84W^6 + 0\left(W^7\right)\right) + \\ &\left(e_0 a\right)^2 \left(\varepsilon_6\left(1 + 6W + 21W^2 + 56W^3 + 126W^4 + 252W^5 + 462W^6 + 0\left(W^7\right)\right)\right) \end{aligned} \right) \end{aligned} \tag{8}$$

Where: I is Moment of inertia, E is Modulus of elasticity, m is Mass of tube per unit length, η is Magnetic fields permeability, H_x is Magnetic fields strength, A is Cross-sectional area, K is foundation stiffness, e_0 is Nonlocal materials constant, a is Internal characteristics length of the tube, w is Displacement, L is Length of the tube, t is Time, x is Cartesian axis, $\bar{h}$ is Plank constant, c is Speed of sound, b is Width of the tube and d is Diameter of the tube.

However, this study analysis dynamic responses of a single walled carbon nanotubes with the following displacements boundaries conditions:

For pinned pinned supports (P-P) tube,

$$w(0,t)=0,\quad \frac{\partial^2 w(0,t)}{\partial^2 x}=0,\quad w(L,t)=0,\quad \frac{\partial^2 w(L,t))}{\partial^2 x}=0. \tag{9}$$

For clamped clamped supports (C-C) tube,

$$w(0,t)=0,\quad \frac{\partial w(0,t)}{\partial x}=0,\quad w((L,t)=0,\quad \frac{\partial w(L,t)}{\partial x}=0. \tag{10}$$

For a clamped pinned supports (C-P) tube,

$$w(0,t)=0,\quad \frac{\partial w(0,t)}{\partial x}=0,\quad w(L,t)=0, \frac{\partial^2 w((L,t)}{\partial^2 x}=0. \tag{11}$$

For a clamped free supports (C-F) tube,

$$w(0,t)=0,\quad \frac{\partial^2 w(0,t)}{\partial x^2}=0,\quad w(L,t)=0, \frac{\partial^3 w((L,t)}{\partial^3 x}=0 \tag{12}$$

Dimensionless variables are;

$$\begin{aligned} &X=\frac{x}{L}, \quad W=\frac{w}{L}, \quad K_1=\frac{k_1L^4}{EI}, \quad \tau=\frac{t}{L^2}\sqrt{\frac{EI}{M}}, \quad H_a=\frac{\eta AH_x^{\ 2}L^2}{EI}, \\ &\varepsilon_6=\frac{e_o^2 a^2\pi^3 hcbL^4}{20EId^6}, \quad \varepsilon_4=\frac{\pi^3 hcbL^4}{240EId^4}, K_3=\frac{k_3L^6}{EI}, \alpha_1=\frac{16d_0^2}{h_2}, \quad K_p=\frac{k_pL^2}{EI}, \quad \theta=\frac{EA\alpha TL^2}{EI} \end{aligned} \tag{13}$$

Applying dimensionless variables of equation (13) into equation (8), yield;

$$\frac{\partial^4 W}{\partial X^4}+\frac{\partial^2 W}{\partial \tau^2}+K_1W+K_3W^3-\left(\theta+H_a+K_p\right)\frac{\partial^2 W}{\partial X^2}-\left(e_0a\right)^2\begin{pmatrix} \frac{\partial^4 W}{\partial X^2\partial \tau^2}+K_1\frac{\partial^2 W}{\partial X^2}+ \\ K_3W^2\frac{\partial^2 W}{\partial X^2}-\begin{pmatrix}\theta+H_a+ \\ K_p\end{pmatrix}\frac{\partial^4 W}{\partial X^4}\end{pmatrix}=$$

$$\begin{pmatrix} \varepsilon_4\left(1+4W+10W^2+20W^3+35W^4+56W^5+84W^6+0\left(W^7\right)\right)+ \\ \left(e_0a\right)^2\left(\varepsilon_6\left(1+6W+21W^2+56W^3+126W^4+252W^5+462W^6+0\left(W^7\right)\right)\right)\end{pmatrix}$$

(14)

Equation (14) is the resulting nonlinear partial differential equations of motion;

Converting Governing Equation from PDE into ode using Galerkin Decomposition Method

For convenience, equation (14) is converted into ordinary differential equation using step-by-step Galerkin decomposition method. This procedure allows the deflection of the CNTs to be represented in the form of product of two independent functions as shown;

$$W\left(X,\tau\right)=V\left(\tau\right)\phi\left(X\right) \tag{15}$$

Where $\phi\left(X\right)$ is the shape function as expressed in table 1, is a function selected to satisfied the boundaries conditions.

Recall that Galerkin one parameter at a time transform is stated as;

Table 1: The basic functions corresponding to above boundaries conditions

Cases	Mode shape, $\phi(x)$	Value of β
1. Simply support 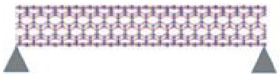	$\sin\left(\frac{\beta x}{L}\right)$	π
2. Clamped-Clamped support 	$\left(\cosh\left(\frac{\beta x}{L}\right)-\cos\left(\frac{\beta x}{L}\right)\right)-\left(\frac{\sinh\beta+\sin\beta}{\cosh\beta-\cos\beta}\right)\left(\sinh\left(\frac{\beta x}{L}\right)-\sin\left(\frac{\beta x}{L}\right)\right)$	4.730041
3. Clamped-Simply support 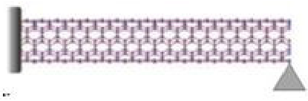	$\left(\cosh\left(\frac{\beta x}{L}\right)-\cos\left(\frac{\beta x}{L}\right)\right)-\left(\frac{\cosh\beta-\cos\beta}{\sinh\beta-\sin\beta}\right)\left(\sinh\left(\frac{\beta x}{L}\right)-\sin\left(\frac{\beta x}{L}\right)\right)$	3.926602
4. Clamped-Free support 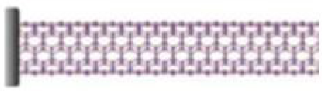	$\left(\cosh\left(\frac{\beta x}{L}\right)-\cos\left(\frac{\beta x}{L}\right)\right)-\left(\frac{\cosh\beta+\cos\beta}{\sinh\beta+\sin\beta}\right)\left(\sinh\left(\frac{\beta x}{L}\right)-\sin\left(\frac{\beta x}{L}\right)\right)$	1.87510

$$\int_0^1 R(X,\tau)\phi(X)\,dX \tag{16}$$

Where $R(X,\tau)$ is the nonlinear equation. Applying equation (16) to the governing nonlinear partial differential equations of motion of equation (14), step-by-step as shown below:

$$\frac{\partial^4 W}{\partial X^4} = \int_0^1 \frac{\partial^4 (V\phi)}{\partial X^4}\phi dx = \left[\int_0^1 \phi \frac{\partial^4 \phi}{\partial X^4}.dx\right] V(t)$$

$$\frac{\partial^2 W}{\partial \tau^2} = \int_0^1 \frac{\partial^2 (V\phi)}{\partial \tau^2}\phi dx = \left[\int_0^1 \phi^2 .dx\right] \ddot{V}(t)$$

$$K_1 W = K_1 \int_0^1 (V\phi)\phi dx = \left[K_1 \int_0^1 \phi^2 dx\right] V(t)$$

$$K_3 W^3 = K_3 \int_0^1 (V\phi)^3 \phi dx = \left[K_3 \int_0^1 \phi^4 dx\right] V^3(t)$$

$$(\theta + H_a + K_p)\frac{d^2 W}{dX^2} = \int_0^1 (\theta + H_a + K_p)\frac{d^2 (V\phi)}{dX^2}\phi dx = \left[(\theta + H_a + K_p)\int_0^1 \phi \frac{d^2\phi}{dX^2}dx\right] V(t)$$

$$(e_0 a)^2 \frac{\partial^4 W}{\partial X^2 \tau^2} = \int_0^1 (e_0 a)^2 \frac{\partial^4 (V\phi)}{\partial X^2 \tau^2}\phi dx = \left[(e_0 a)^2 \int_0^1 \phi \frac{\partial^2 \phi}{\partial X^2}dx\right] \ddot{V}(t)$$

$$(e_0 a)^2 K_1 \frac{\partial^2 W}{\partial X^2} = \int_0^1 (e_0 a)^2 K_1 \frac{\partial^2 (V\phi)}{\partial X^2}\phi dx = \left[(e_0 a)^2 K_1 \int_0^1 \phi \frac{\partial^2 \phi}{\partial X^2}dx\right] V(t)$$

$$(e_0 a)^2 K_3 W^2 \frac{\partial^2 W}{\partial X^2} = \int_0^1 (e_0 a)^2 K_3 (V\phi)^2 \frac{\partial^2 (V\phi)}{\partial X^2}\phi dx = \left[(e_0 a)^2 K_3 \int_0^1 \phi^3 \frac{\partial^2 \phi}{\partial X^2}dx\right] V^3(t)$$

$$(\theta + H_a + K_p)\frac{d^4 W}{dX^4} = \int_0^1 (\theta + H_a + K_p)\frac{d^4 (V\phi)}{dX^4}\phi dx = \left[(\theta + H_a + K_p)\int_0^1 \phi \frac{d^4\phi}{dX^4}dx\right] V(t)$$

$$\varepsilon_4 + \varepsilon_6 = \int_0^1 (\varepsilon_4 + \varepsilon_6)\phi dx = \left[\int_0^1 (\varepsilon_4 + \varepsilon_6)\phi dx\right] V(t)$$

$$(4\varepsilon_4 + 10\varepsilon_6) W = \int_0^1 (4\varepsilon_4 + 10\varepsilon_6)(V\phi)\phi dx = \left[\int_0^1 (4\varepsilon_4 + 10\varepsilon_6)\phi^2 dx\right] V(t)$$

$$(10\varepsilon_4 + 21\varepsilon_6) W^2 = \int_0^1 (10\varepsilon_4 + 21\varepsilon_6)(V\phi)^2 \phi dx = \left[\int_0^1 (10\varepsilon_4 + 21\varepsilon_6)\phi^3 dx\right] V^2(t)$$

$$(20\varepsilon_4 + 56\varepsilon_6) W^3 = \int_0^1 (20\varepsilon_4 + 56\varepsilon_6)(V\phi)^3 \phi dx = \left[\int_0^1 (20\varepsilon_4 + 56\varepsilon_6)\phi^4 dx\right] V^3(t)$$

$$(35\varepsilon_4 + 126\varepsilon_6)W^4 = \int_0^1 (35\varepsilon_4 + 126\varepsilon_6)(V\phi)^4 \phi dx = \left[\int_0^1 (35\varepsilon_4 + 126\varepsilon_{66})\phi^5 dx\right] V^4(t)$$

$$(56\varepsilon_4 + 252\varepsilon_6)W^5 = \int_0^1 (56\varepsilon_4 + 252\varepsilon_6)(V\phi)^5 \phi dx = \left[\int_0^1 (56\varepsilon_4 + 252\varepsilon_6)\phi^6 dx\right] V^5(t)$$

$$(84\varepsilon_4 + 462\varepsilon_6)W^6 = \int_0^1 (84\varepsilon_4 + 462\varepsilon_6)(V\phi)^6 \phi dx = \left[\int_0^1 (84\varepsilon_4 + 462\varepsilon_6)\phi^7 dx\right] V^6(t)$$

Therefore, the Ordinary Differential Equation (ODE) is arrived as:

$$M\ddot{V} + \alpha_0 + \alpha_1 V + \alpha_2 V^2 + \alpha_3 V^3 + \alpha_4 V^4 + \alpha_5 V^5 + \alpha_6 V^6 = 0 \quad (17)$$

Where the coefficient is defined as:

$$M = \int_0^1 \left[\phi + (e_0 a)^2 \frac{d^2\phi(X)}{dX^2}\right]\phi(X)dX$$

$$\alpha_0 = \int_0^1 [(\varepsilon_4 + \varepsilon_6)]\phi(X)dX$$

$$\alpha_1 = \int_0^1 \left[\frac{d^4\phi(X)}{dX^4} + K_1\phi(X) + (\theta + H_a + K_p)\frac{d^2\phi(X)}{dX^2} + (e_0 a)^2 K_1 \frac{d^2\phi(X)}{dX^2} + (\theta + H_a + K_p)\frac{d^4\phi(X)}{dX^4} + (4\varepsilon_4 + 10\varepsilon_6)\phi(X)\right]\phi(X)dX$$

$$\alpha_2 = \int_0^1 [(10\varepsilon_4 + 216\varepsilon_6)]\phi^3(X)dX$$

$$\alpha_3 = \int_0^1 \left[K_3\phi^3(X) + (e_0 a)^2 K_3 \phi^2(X)\frac{d^2\phi(X)}{dX^2} + (20\varepsilon_4 + 56\varepsilon_6)\phi^3(X)\right]\phi(X)dX$$

$$\alpha_4 = \int_0^1 [(35\varepsilon_4 + 126\varepsilon_6)]\phi^5(X)dX$$

$$\alpha_5 = \int_0^1 [(56\varepsilon_4 + 252\varepsilon_6)]\phi^6(X)dX$$

$$\alpha_6 = \int_0^1 [(84\varepsilon_4 + 462\varepsilon_6)]\phi^7(X)dX$$

Method of Solutions

The homotopic perturbation method was first introduced by Ji Huan, in 1998. This method becomes famous and more acceptable as an elegance tool in the hand of several researchers due to it simplicity in nature and gives rise to high effective solution of complex nonlinear problem in several diversify areas of sciences and technological based knowledge. To illustrate this general procedure, consider a general nonlinear partial differential equation of the forms;

$$A(u) - f(r) = 0, r \in \Omega \quad (18)$$

Subjected to boundary condition:

$$B\left(u, \frac{\partial u}{\partial n}\right) = 0, r \in \Gamma, \quad (19)$$

where A is a general differential operator, B a boundary operator, $f(r)$ a known analytical function and Γ is the boundary of the domain Ω. In general, one can divide the operator A into two parts: linear and non- linear. That means

$$\mathrm{A} = L + \mathrm{N} \tag{20}$$

where L is linear and N is non-linear.

Hence, equation (2.1) can now be rewritten as

$$L(u) + \mathrm{N}(u) - f(r) = 0, r \in \Omega \tag{21}$$

By the homotopy technique, one can construct a homotopy in the following way $v(r, p) : \Omega x[0,1] \rightarrow R$ which satisfies

$$\mathrm{H}(v, p) = (1-p)\left[L(v) - L(u_0)\right] + p\left[\mathrm{A}(v) - f(r)\right] = 0, \qquad p \in [0,1], r \in \Omega \tag{22}$$

Or

$$\mathrm{H}(v, p) = L(v) - L(u_0) + p\left[\mathrm{N}(v) - f(r)\right] = 0 \tag{23}$$

where $p \in [0,1]$] is an embedding parameter, u_0 is an initial approximation which satisfies the boundary conditions.

$$H(v, 0) = L(v) - L(u_0) = 0 \tag{24}$$

$$H(v, 1) = \mathrm{A}(v) - f(r) = 0 \tag{25}$$

The changing process of p from zero to unity is just that of $v(r, p)$ from $u_0(r)$ to $u(r)$. In topology, this is called deformation and $L(v) - L(u_0)$ and $\mathrm{A}(v) - f(r)$ are called homotopy. According to the HPM, we can first use the embedding parameter p as a "small parameter" and assume that the solution be written as a power series in p

$$v = v_o + pv_1 + p^2 v_2 + \ldots \tag{26}$$

Let $p = 1$, result in the approximate solutions:

$$u = \lim_{p \to 1} v = v_0 + v_1 + v_2 + \ldots \tag{27}$$

The combination of the perturbation and homotopic method is called the homotopy perturbation method (HPM), which has eliminated limitations of the traditional perturbation methods. On the other hand, this method has full merit of the traditional perturbation method.

Applying homotopy perturbation method on ordinary differential equation of equation (17) and divide through by m yield;

$$\ddot{V} + \frac{\alpha_0}{m} + \frac{\alpha_1}{m}V + \frac{\alpha_2}{m}V^2 + \frac{\alpha_3}{m}V^3 + \frac{\alpha_4}{m}V^4 + \frac{\alpha_5}{m}V^5 + \frac{\alpha_6}{m}V^6 = 0 \tag{28}$$

$$\text{Let, } \beta_0 = \frac{\alpha_0}{m}, \beta_1 = \frac{\alpha_1}{m}, \beta_2 = \frac{\alpha_2}{m}, \beta_3 = \frac{\alpha_3}{m}, \beta_4 = \frac{\alpha_4}{m}, \beta_5 = \frac{\alpha_5}{m}, \beta_6 = \frac{\alpha_6}{m}, \tag{29}$$

Substitute equation (33) into equation (32) gives;

$$\ddot{V} + \beta_0 + \beta_1 V + \beta_2 V^2 + \beta_3 V^3 + \beta_4 V^4 + \beta_5 V^5 + \beta_6 V^6 = 0 \tag{30}$$

Apply, HPM on equation (34) becomes:

$$\mathrm{H}(v,p)=(1-p)\left[\ddot{V}+\beta_1 V\right]+p\left[\ddot{V}+\beta_0+\beta_1 V+\beta_2 V^2+\beta_3 V^3+\beta_4 V^4+\beta_5 V^5+\beta_6 V^6\right]=0 \quad (31)$$

$$p\in[0,1], r\in\Omega$$

Perturbating the parameters become (32) & (33) are obtain as follows;

$$\left.\begin{aligned}\ddot{V}&=V_0^{''}+pV_1^{''}+p^2V_2^{''}+\dots\\ \dot{V}&=V_0^{'}+pV_1^{'}+p^2V_2^{'}+\dots\\ V&=V_0+pV_1+p^2V_2+\dots\end{aligned}\right\} \quad (32)$$

And

$$\beta_1=\omega_0^2+p\omega_1^2+p^2\omega_2^2+\dots \quad (33)$$

Substitute equation (32) & (33) into equation (31), yield;

$$\left\{\begin{array}{l}(1-p)\left[V_0^{''}+pV_1^{''}+p^2V_2^{''}+\dots+\left(\omega_0^2+p\omega_1^2+p^2\omega_2^2+\dots\right)\left(V_0+pV_1+p^2V_2+\dots\right)\right]+\\ p\left[\begin{array}{l}V_0^{''}+pV_1^{''}+p^2V_2^{''}+\dots+\left(\omega_0^2+p\omega_1^2+p^2\omega_2^2+\dots\right)\left(V_0+pV_1+p^2V_2+\dots\right)+\\ \beta_2\left(V_0+pV_1+p^2V_2+\dots\right)^2+\beta_3\left(V_0+pV_1+p^2V_2+\dots\right)^3+\\ \beta_4\left(V_0+pV_1+p^2V_2+\dots\right)^4+\beta_5\left(V_0+pV_1+p^2V_2+\dots\right)^5+\beta_6\left(\begin{array}{l}V_0+pV_1+\\ p^2V_2+\dots\end{array}\right)^6+\beta_0\end{array}\right]\end{array}\right\}=0$$

(34)

Expanding equation (34) and collecting all terms with the same order of p together, the following resulting equations appears in form of polynomial in power of p are obtain. Where, u_i and ω_i^2, $i=0,1,2,\dots$ and equated same to zero as shown below;

$$\mathrm{P}^0: V_0^{''}+\omega_0^2V_0=0 \quad (35)$$

Subject to: $U_0(0)=\mathrm{A}$ and $\dot{U}_0(0)=0$

$$\mathrm{P}^1: V_1^{''}+\omega_0^2V_1+\omega_1^2V_0+\beta_2V_0^2+\beta_2V_0^3+\beta_2V_0^4+\beta_2V_0^5+\beta_2V_0^6+\beta_0=0 \quad (36)$$

Subject to: $U_1(0)=0$ and $\dot{U}_1(0)=0$

Using initial conditions in equation (35) which give the solution as;

$$V_0=A\cos(\omega_0 t) \quad (37)$$

Substituting the value of equation (37) into equation (36) yields;

$$\left(\begin{array}{l}V_1^{''}+\omega_0^2V_1+\omega_1^2\left(A\cos\omega_0 t\right)+\beta_2(A\cos\omega_0 t)^2+\beta_3(A\cos\omega_0 t)^3+\\ \beta_4(A\cos\omega_0 t)^4+\beta_5(A\cos\omega_0 t)^5+\beta_6(A\cos\omega_0 t)^6+\beta_0\end{array}\right)=0 \quad (38)$$

Performing trigonometric identities function on equation (38) gives;

$$\begin{pmatrix} \ddot{V}(t)+\omega_0^2 V(t)_1+\omega_1^2 A\cos(\omega t)+\frac{\beta_2 A^2}{2}\cos(2\omega t)+\frac{\beta_2 A^2}{2}+\frac{\beta_3 A^3}{4}\cos(3\omega t)+ \\ \frac{3\beta_3 A^3}{4}\cos(\omega t)+\frac{\beta_4 A^4}{8}\cos(4\omega t)+\frac{\beta_4 A^4}{2}\cos(2\omega t)+ \\ \frac{3\beta_4 A^4}{8}+\frac{\beta_5 A^5}{16}\cos(5\omega t)+\frac{5\beta_5 A^5\cos(3\omega t)}{16}+\frac{5\beta_5 A^5}{8}\cos(\omega t)+ \\ \frac{\beta_6 A^6}{32}\cos(6\omega t)+\frac{3\beta_6 A^6}{16}\cos(4\omega t)+\frac{15\beta_6 A^6\cos(2\omega t)}{32}+\frac{5\beta_6 A^6}{16}+\beta_0=0 \end{pmatrix} \tag{39}$$

Neglecting secular terms in equation (39) becomes;

$$\left(\omega_1^2 A+\frac{3\beta_3 A^3}{4}+\frac{5\beta_5 A^5}{8}\right)\cos(\omega t)=0 \tag{40}$$

And natural nonlinear frequency ω_1 is obtained as $\omega_1=\sqrt{-\left(\frac{3\beta_3 A^2}{4}+\frac{5\beta_5 A^4}{8}\right)}$ (41)

For the Model Stability Analysis

From equation (33), setting $p=1$, $\beta_1=\omega_0^2+\omega_1^2+\ldots=0$ (42)

Substitute ω_1^2 into equation (41), gives:

$$\beta_1=\omega_0^2-\frac{3\beta_3 A^2}{4}-\frac{5\beta_5 A^4}{8} \tag{43}$$

$$\omega_0=\sqrt{\beta_1+\frac{3\beta_3 A^2}{4}+-\frac{5\beta_5 A^4}{8}} \tag{44}$$

Natural frequency is obtained as;

$$\omega_n=\sqrt{\frac{\alpha_1}{m}}=\sqrt{\beta_1} \tag{45}$$

Therefore, frequency ratio is obtained as;

$$\frac{\omega_0}{\omega_n}=\frac{\sqrt{\beta_1+\frac{3\beta_3 A^2}{4}+-\frac{5\beta_5 A^4}{8}}}{\sqrt{\beta_1}}=\sqrt{1+\frac{1}{\beta_1}\left(\frac{3\beta_3 A^2}{4}+-\frac{5\beta_5 A^4}{8}\right)} \tag{46}$$

Substituting gives;

$$\frac{\omega_0}{\omega_n} = \sqrt{1 + 4\mathrm{A}^2\left(\frac{3\alpha_3 + 10\alpha_5 \mathrm{A}^2}{\alpha_1}\right)} \tag{47}$$

Substituting yields;

$$\frac{\omega_0}{\omega_n} = \sqrt{1 + 4A^2\left(\frac{\left(3\int_0^1\left[K_3\phi^3(X) + (e_0a)^2 K_3\phi^2\frac{d^2\phi(X)}{dX^2} + (20\varepsilon_4 + 56\varepsilon_6)\phi^3\right]\phi(X)\,dX + 10A^2\int_0^1[(56\varepsilon_4 + 126\varepsilon_6)]\phi^6(X)\,dX\right)}{\int_0^1\left[\begin{array}{l}\frac{d^4\phi(X)}{dX^4} + K_1\phi(X) + (\theta + H_a + K_p)\frac{d^2\phi(X)}{dX^2} + (e_0a)^2 K_1\frac{d^2\phi(X)}{dX^2} + \\ (\theta + H_a + K_p)\frac{d^4\phi(X)}{dX^4} + (4\varepsilon_4 + 10\varepsilon_6)\end{array}\right]\phi(X)\,dX}\right)} \tag{48}$$

Solving equation (39) and neglecting secular terms with the boundary conditions;

$$V_1(t) = \frac{1}{1680\omega_0^2}\left(\begin{array}{l}48A^6(\cos(\omega_0 t))^6\beta_6 + 96\beta_6 A^6(\cos(\omega_0 t))^4 + \\ 350A^5(\cos(\omega_0 t))^5\beta_5 + 384A^6\beta_6(\cos(\omega_0 t))^2 - \\ 175A^5(\cos(\omega_0 t))^3\beta_5 + 112A^4(\cos(\omega_0 t))^4\beta_4 + \\ 240A^6\cos(\omega_0 t)\beta_6 - 768\beta_6 A^6 - 175\beta_5 A^5\cos(\omega_0 t) + \\ 448A^4\beta_4(\cos(\omega_0 t))^2 + 630A^3(\cos(\omega_0 t))^3\beta_3 + \\ 336A^4\cos(\omega_0 t)\beta_4 - 896A^4\beta_4 - 630\beta_3 A^3\cos(\omega_0 t) + \\ 560A^2(\cos(\omega_0 t))^2\beta_2 + 560A^2\cos(\omega_0 t)\beta_2 - \\ 1120\beta_2 A^2 + 1680\cos(\omega_0 t)\beta_0 - 1680\beta_0\end{array}\right) \tag{49}$$

Adding the series solutions yield;

$$V(t) = V_0(t) + V_1(t) + \ldots \tag{50}$$

$$V(t) = \left(A\cos(\omega_0 t) + \frac{1}{1680\omega_0^2}\left(\begin{array}{l}48A^6(\cos(\omega_0 t))^6\beta_6 + 96\beta_6 A^6(\cos(\omega_0 t))^4 + \\ 350A^5(\cos(\omega_0 t))^5\beta_5 + 384A^6\beta_6(\cos(\omega_0 t))^2 - \\ 175A^5(\cos(\omega_0 t))^3\beta_5 + 112A^4(\cos(\omega_0 t))^4\beta_4 + \\ 240A^6\cos(\omega_0 t)\beta_6 - 768\beta_6 A^6 - 175\beta_5 A^5\cos(\omega_0 t) + \\ 448A^4\beta_4(\cos(\omega_0 t))^2 + 630A^3(\cos(\omega_0 t))^3\beta_3 + \\ 336A^4\cos(\omega_0 t)\beta_4 - 896A^4\beta_4 - 630\beta_3 A^3\cos(\omega_0 t) + \\ 560A^2(\cos(\omega_0 t))^2\beta_2 + 560A^2\cos(\omega_0 t)\beta_2 - \\ 1120\beta_2 A^2 + 1680\cos(\omega_0 t)\beta_0 - 1680\beta_0\end{array}\right)\right) + \ldots \tag{51}$$

Therefore, deflection for each of four boundary conditions are obtained using equation (15) above;

For pinned-pinned supports (P-P), deflection becomes;

$$w(x,t)=\left[\begin{array}{l} A\cos(\omega_0 t)+ \\ \dfrac{1}{1680\omega_0^2}\left(\begin{array}{l} 48A^6\left(\cos(\omega_0 t)\right)^6\beta_6+96\beta_6A^6\left(\cos(\omega_0 t)\right)^4+ \\ 350A^5\left(\cos(\omega_0 t)\right)^5\beta_5+384A^6\beta_6\left(\cos(\omega_0 t)\right)^2- \\ 175A^5\left(\cos(\omega_0 t)\right)^3\beta_5+112A^4\left(\cos(\omega_0 t)\right)^4\beta_4+ \\ 240A^6\cos(\omega_0 t)\beta_6-768\beta_6A^6-175\beta_5A^5\cos(\omega_0 t)+ \\ 448A^4\beta_4\left(\cos(\omega_0 t)\right)^2+630A^3\left(\cos(\omega_0 t)\right)^3\beta_3+ \\ 336A^4\cos(\omega_0 t)\beta_4-896A^4\beta_4-630\beta_3A^3\cos(\omega_0 t)+ \\ 560A^2\left(\cos(\omega_0 t)\right)^2\beta_2+560A^2\cos(\omega_0 t)\beta_2- \\ 1120\beta_2A^2+1680\cos(\omega_0 t)\beta_0-1680\beta_0 \end{array}\right) \end{array}\right]*\sin\left(\frac{\beta x}{l}\right) \quad (52)$$

For clamped-clamped supports (C-C), deflection becomes;

$$w(x,t)=\left[\begin{array}{l} A\cos(\omega_0 t) \\ +\dfrac{1}{1680\omega_0^2}\left(\begin{array}{l} 48A^6\left(\cos(\omega_0 t)\right)^6\beta_6+96\beta_6A^6\left(\cos(\omega_0 t)\right)^4 \\ +350A^5\left(\cos(\omega_0 t)\right)^5\beta_5+384A^6\beta_6\left(\cos(\omega_0 t)\right)^2 \\ -175A^5\left(\cos(\omega_0 t)\right)^3\beta_5+112A^4\left(\cos(\omega_0 t)\right)^4\beta_4 \\ +240A^6\cos(\omega_0 t)\beta_6-768\beta_6A^6-175\beta_5A^5\cos(\omega_0 t) \\ +448A^4\beta_4\left(\cos(\omega_0 t)\right)^2+630A^3\left(\cos(\omega_0 t)\right)^3\beta_3 \\ +336A^4\cos(\omega_0 t)\beta_4-896\beta_4A^4-630\beta_3A^3\cos(\omega_0 t) \\ +560A^2\left(\cos(\omega_0 t)\right)^2\beta_2+560A^2\cos(\omega_0 t)\beta_2 \\ -1120\beta_2A^2+1680\cos(\omega_0 t)\beta_0-1680\beta_0 \end{array}\right) \end{array}\right]*\left(\begin{array}{l} \cosh\left(\dfrac{\beta x}{l}\right)-\cos\left(\dfrac{\beta x}{l}\right) \\ -\dfrac{\sinh(\beta)+\sin(\beta)}{\cosh(\beta)-\cos(\beta)} \\ \left(\sinh\left(\dfrac{\beta x}{l}\right)-\sin\left(\dfrac{\beta x}{l}\right)\right) \end{array}\right) \quad (53)$$

For clamped-pinned supports (C-P), deflection becomes;

$$w(x,t)=\left[\begin{array}{l} A\cos(\omega_0 t) \\ +\dfrac{1}{1680\omega_0^2}\left(\begin{array}{l} 48A^6\left(\cos(\omega_0 t)\right)^6\beta_6+96\beta_6A^6\left(\cos(\omega_0 t)\right)^4 \\ +350A^5\left(\cos(\omega_0 t)\right)^5\beta_5+384A^6\beta_6\left(\cos(\omega_0 t)\right)^2 \\ -175A^5\left(\cos(\omega_0 t)\right)^3\beta_5+112A^4\left(\cos(\omega_0 t)\right)^4\beta_4 \\ +240A^6\cos(\omega_0 t)\beta_6-768\beta_6A^6-175\beta_5A^5\cos(\omega_0 t) \\ +448A^4\beta_4\left(\cos(\omega_0 t)\right)^2+630A^3\left(\cos(\omega_0 t)\right)^3\beta_3 \\ +336A^4\cos(\omega_0 t)\beta_4-896\beta_4A^4-630\beta_3A^3\cos(\omega_0 t) \\ +560A^2\left(\cos(\omega_0 t)\right)^2\beta_2+560A^2\cos(\omega_0 t)\beta_2 \\ -1120\beta_2A^2+1680\cos(\omega_0 t)\beta_0-1680\beta_0 \end{array}\right) \end{array}\right]*\left(\begin{array}{l} \cosh\left(\dfrac{\beta x}{l}\right)-\cos\left(\dfrac{\beta x}{l}\right) \\ -\dfrac{\cosh(\beta)-\cos(\beta)}{\sinh(\beta)-\sin(\beta)} \\ \left(\sinh\left(\dfrac{\beta x}{l}\right)-\sin\left(\dfrac{\beta x}{l}\right)\right) \end{array}\right) \quad (54)$$

For clamped-free supports (C-F), deflection becomes;

$$w(x,t)=\left[\begin{array}{l} A\cos(\omega_0 t) \\ +\dfrac{1}{1680\omega_0^2}\left(\begin{array}{l} 48A^6(\cos(\omega_0 t))^6\beta_6+96\beta_6A^6(\cos(\omega_0 t))^4 \\ +350A^5(\cos(\omega_0 t))^5\beta_5+384A^6\beta_6(\cos(\omega_0 t))^2 \\ -175A^5(\cos(\omega_0 t))^3\beta_5+112A^4(\cos(\omega_0 t))^4\beta_4 \\ +240A^6\cos(\omega_0 t)\beta_6-768\beta_6A^6-175\beta_5A^5\cos(\omega_0 t) \\ +448A^4\beta_4(\cos(\omega_0 t))^2+630A^3(\cos(\omega_0 t))^3\beta_3 \\ +336A^4\cos(\omega_0 t)\beta_4-896\beta_4A^4-630\beta_3A^3\cos(\omega_0 t) \\ +560A^2(\cos(\omega_0 t))^2\beta_2+560A^2\cos(\omega_0 t)\beta_2 \\ -1120\beta_2A^2+1680\cos(\omega_0 t)\beta_0-1680\beta_0 \end{array}\right) \end{array}\right] * \left(\begin{array}{l} \cosh\left(\dfrac{\beta x}{l}\right)-\cos\left(\dfrac{\beta x}{l}\right) \\ -\dfrac{\cosh(\beta)+\cos(\beta)}{\sinh(\beta)+\sin(\beta)} \\ \left(\sinh\left(\dfrac{\beta x}{l}\right)-\sin\left(\dfrac{\beta x}{l}\right)\right) \end{array}\right) \quad (55)$$

Results and Discussion

Effect of Thermal Term on Frequency Ratio-Amplitude Curves for Different End Conditions

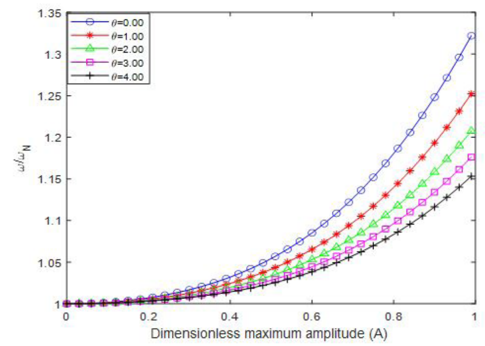

Figure 1: Show effects of thermal term on nondimensional amplitude-frequency ratio on pinned-pinned supports

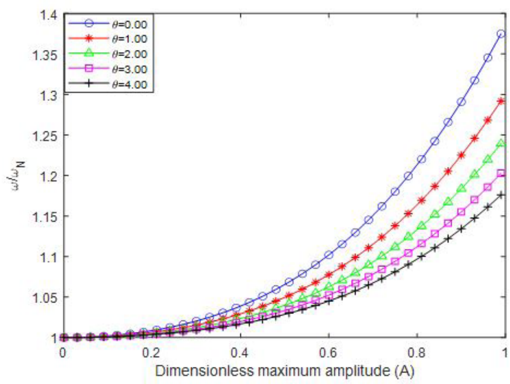

Figure 2: Show effects of thermal term on nondimensional amplitude-frequency ratio amplitude-frequency ratio on clamped-clamped supports

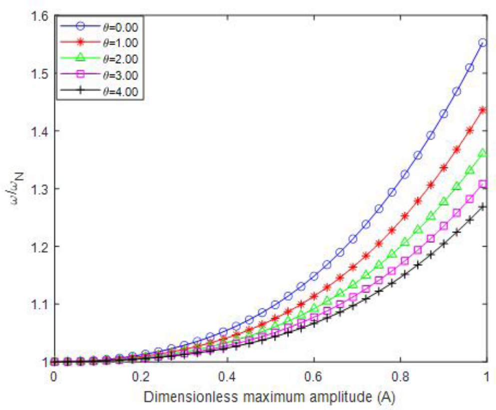

Figure 3: Show effects of thermal term on nondimensional amplitude-frequency ratio amplitude-frequency ratio on clamped-pinned supports

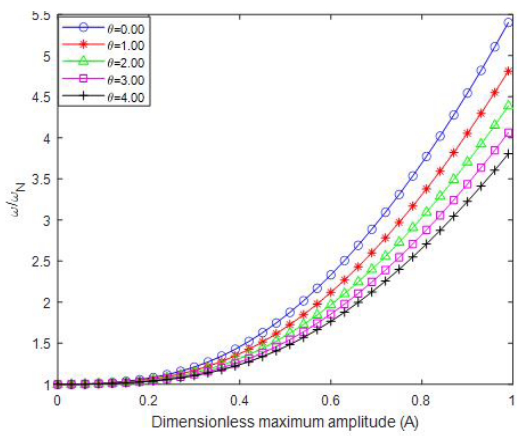

Figure 4: Show effects of thermal term on nondimensional amplitude-frequency ratio amplitude-frequency ratio on clamped-free supports

Figure 1, 2, 3 and 4 show influences of thermal term of different boundaries conditions on nondimensional amplitude-frequency ratio curve of vibration of single walled carbon nanotube resting on spring medium with magnetic and thermal effects under the influence of Casimir force. However, the figures show that, as thermal term increase from zero to maximum values frequency-ratio decrease towards linear system. This shows that for CNTs structure to gained stability, thermal term must be kept at both maximum.

Effect of Linear Foundation Coefficient on Frequency Ratio-amplitude Curves For Different End Conditions

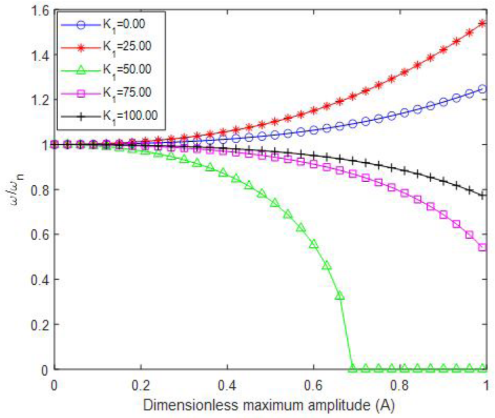

Figure 5: show effects of linear Winkler foundation term on nondimensional amplitude-frequency ratio on pinned-pinned supports

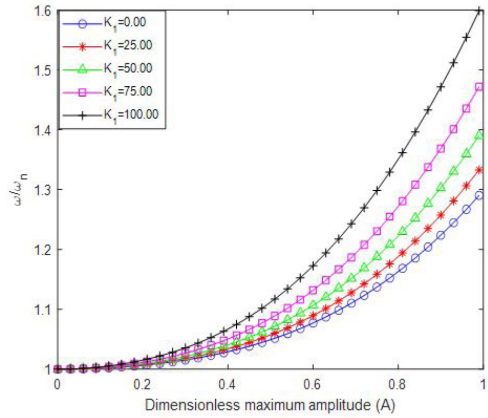

Figure 6: show effects of linear Winkler foundation term on nondimensional amplitude-frequency ratio on clamped-clamped supports

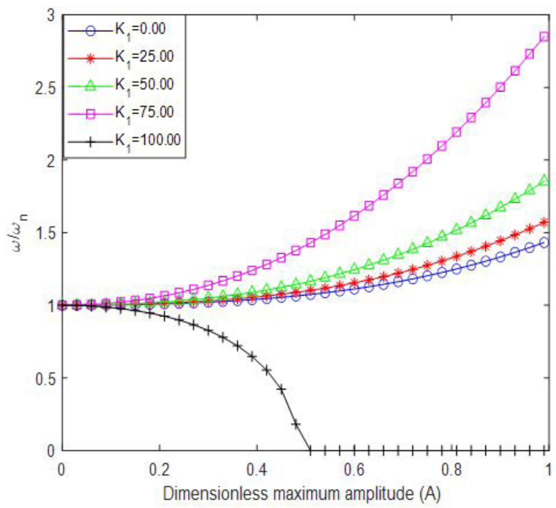

Figure 7: show effects of linear Winkler foundation term on nondimensional amplitude-frequency ratio on clamped-pinned supports

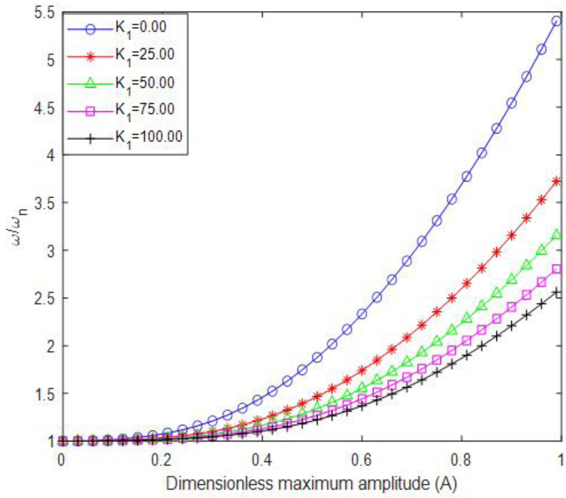

Figure 8: show effects of linear Winkler foundation term on nondimensional amplitude-frequency ratio on clamped-free supports

Figure 5, 6, 7 and 8 show influence of different boundary conditions of linear Winkler-type elastic medium on nondimensional amplitude-frequency ratio curve of vibration of single walled carbon nanotubes resting on elastic foundation with magnetic and thermal effects under the influence of Casimir force. However, figure 5 depict that, linear Winkler elastic medium increase from zero to maximum, its corresponding frequency-ratio decrease towards linear system. Figure 6 depict that, linear Winkler elastic medium increase from zero to maximum, frequency-ratio increase as well. Figure 7 depict that, linear Winkler elastic medium increase from zero to maximum, frequency-ratio increases and decreases toward linear system when the Winkler medium is 100. Figure 8 depict that, linear Winkler elastic medium increases from zero to maximum, frequency-ratio decrease towards linear system. Which mean that the stability should be kept at maximum in selecting foundation.

Effect of Nonlinear Foundation Constant on Frequency Ratio-Amplitude Curves for Different End Conditions

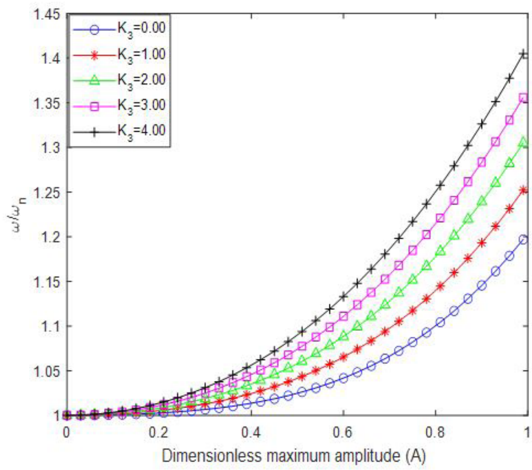

Figure 9: show effects of nonlinear Winkler foundation term on nondimensional amplitude-frequency ratio on pinned-pinned supports

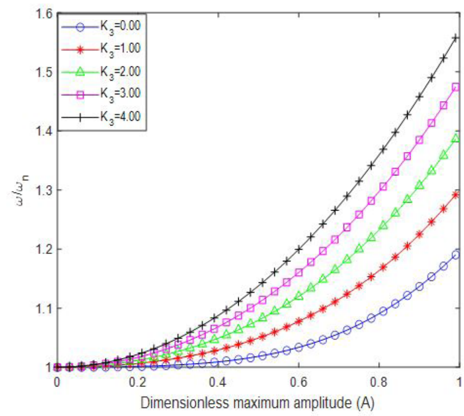

Figure 10: show effects of nonlinear Winkler foundation term on nondimensional amplitude-frequency ratio on clamped-clamped supports

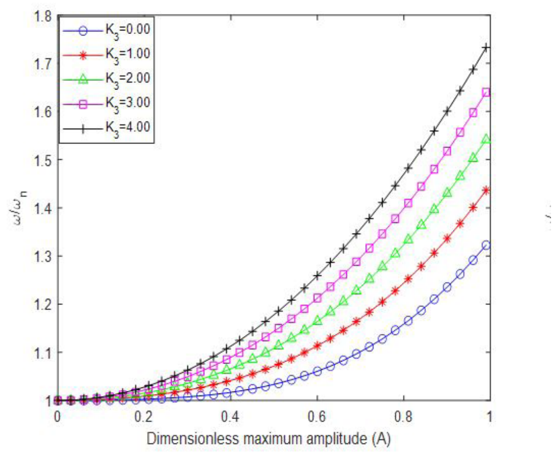

Figure 11: show effects of nonlinear Winkler foundation term on nondimensional amplitude-frequency ratio on clamped-pinned supports

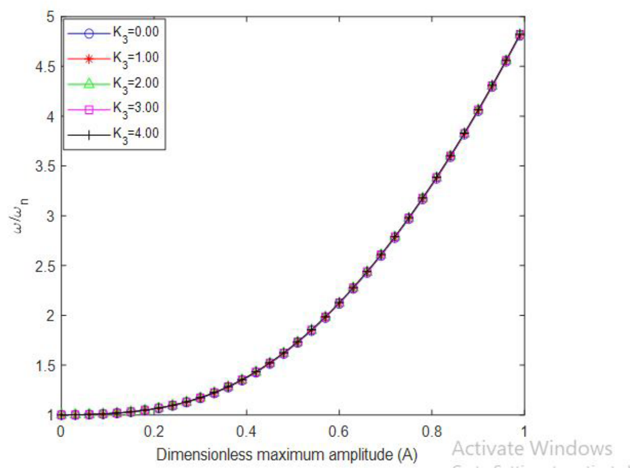

Figure 12: show effects of nonlinear Winkler foundation term on nondimensional amplitude-frequency ratio on clamped-free supports

Figure 9, 10, 11 and 12 show influence of different boundary conditions of nonlinear Winkler elastic medium on nondimensional amplitude-frequency ratio curve of vibration of single-walled carbon nanotubes resting on elastic foundation with magnetic and thermal effects under the influence of Casimir force. Figure 9, 10, 11 and 12 depict that as nonlinear Winkler elastic medium increase from zero to maximum, there is corresponding increase in frequency-ratio except for clamped-free supports which remain constants despite the increase in nonlinear Winkler foundation. This shows that for CNTs structure to gained stability, nonlinear Winkler elastic foundation must be kept at minimum.

Effect of Pasternak Foundation Constant on Frequency Ratio-Amplitude Curves for Different End Conditions

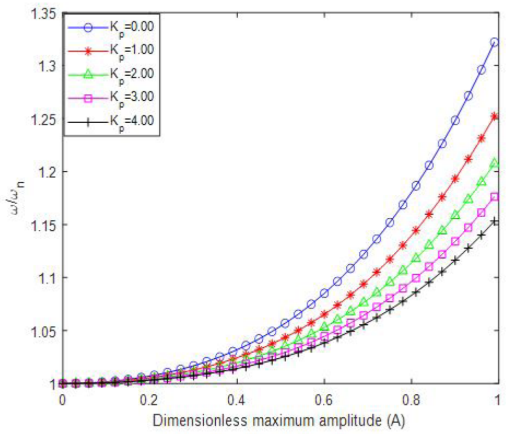

Figure 13: show effects of Pasternak foundation term on nondimensional amplitude-frequency ratio on pinned-pinned supports

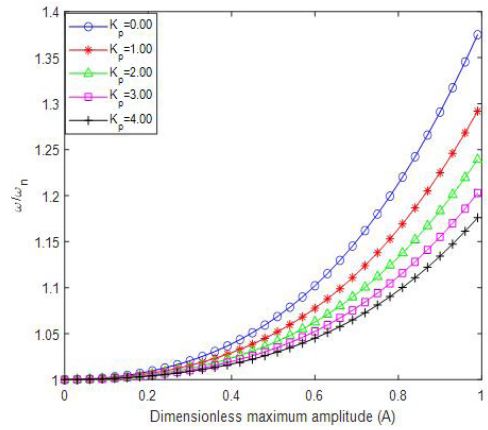

Figure 14: show effects of Pasternak foundation term on nondimensional amplitude-frequency ratio on clamped-clamped supports

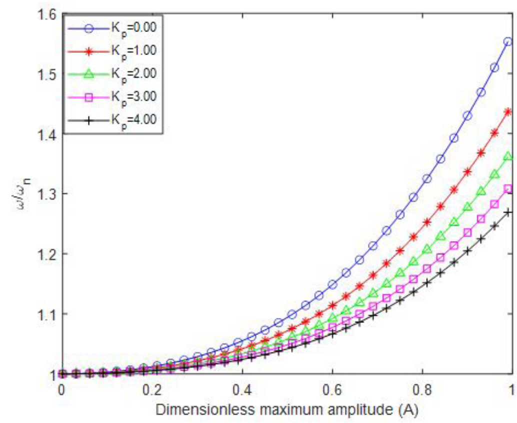

Figure 15 : Show effects of Pasternak foundation term on nondimensional amplitude-frequency ratio on clamped-pinned supports

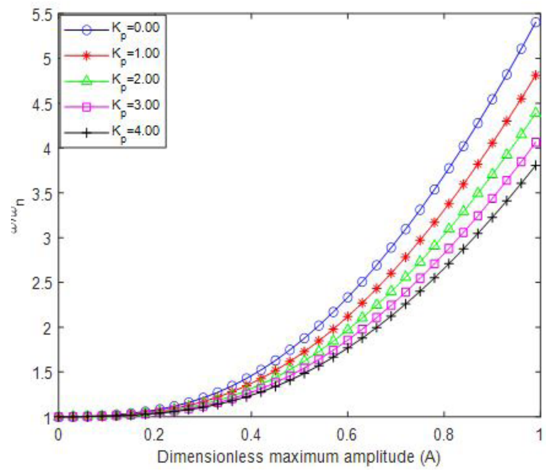

Figure 16: show effects of Pasternak foundation term on nondimensional amplitude-frequency ratio on clamped-free supports

Figure 13, 14, 15 and 16 show influence of Pasternak elastic medium of different boundaries conditions on nondimensional amplitude-frequency ratio curve of vibration of single walled carbon nanotubes resting on elastic footing with magnetic and thermal effects under the influence of Casimir force. Figure 13, 14, 15 and 16 depict that as Pasternak elastic medium increase from zero to maximum, frequency-ratio decrease towards linear system. This shows that for this single walled carbon nanotubes structure to gained stability, Pasternak elastic medium must be kept maximum.

Effect of Magnetic Term on Frequency Ratio-Amplitude Curves for Different End Conditions

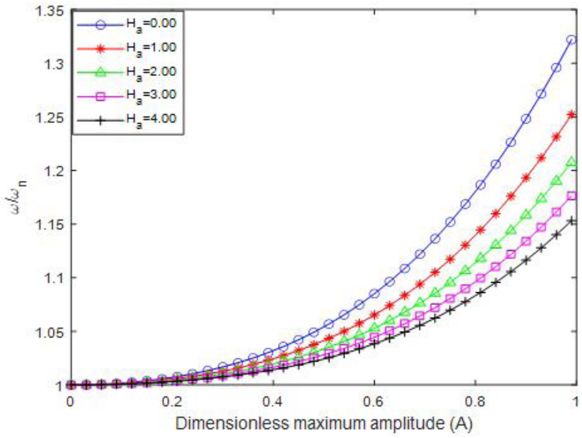

Figure 17: show effects of magnetic term on nondimensional amplitude-frequency ratio on pinned-pinned supports

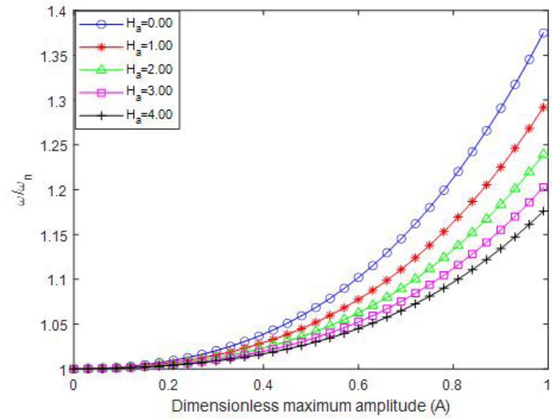

Figure 18: show effects of magnetic term on nondimensional amplitude-frequency ratio on clamped-clamped supports

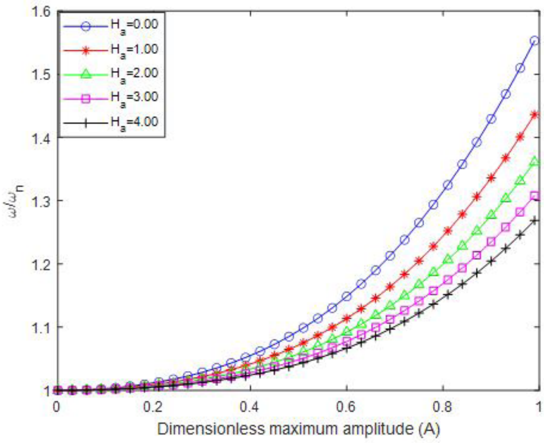

Figure 19: show effects of magnetic term on nondimensional amplitude-frequency ratio on clamped-pinned supports

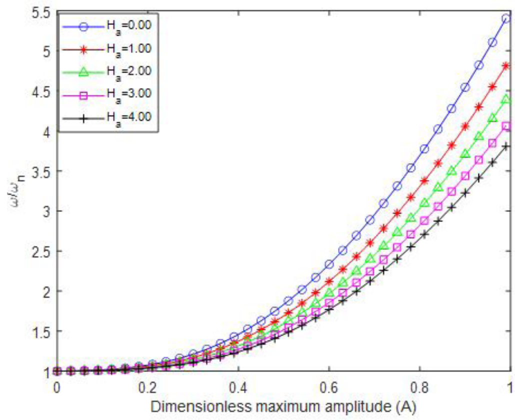

Figure 20: show effects of magnetic term on nondimensional amplitude-frequency ratio on clamped-free supports

Figure 17, 18, 19 and 20 show influence of different boundaries conditions of magnetic term on nondimensional amplitude-frequency ratio curve of vibration of single walled carbon nanotubes resting on elastic foundation with magnetic and thermal effects under the influence of Casimir force. Figures depict that, magnetic term increase from zero to maximum, its corresponding frequency-ratio decrease towards linear system. This shows that for single walled carbon nanotube structure to gained stability, magnetic term must be kept at maximum.

Effect of Nonlocal Term on Frequency Ratio-Amplitude Curves for Different End Conditions

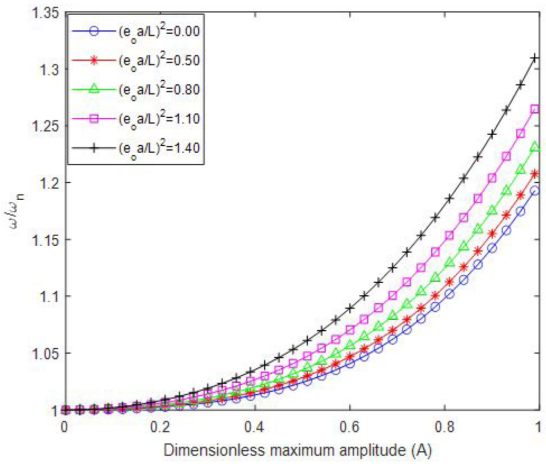

Figure 21 show effects of nonlocal parameter on nondimensional amplitude-frequency ratio on pinned-pinned supports

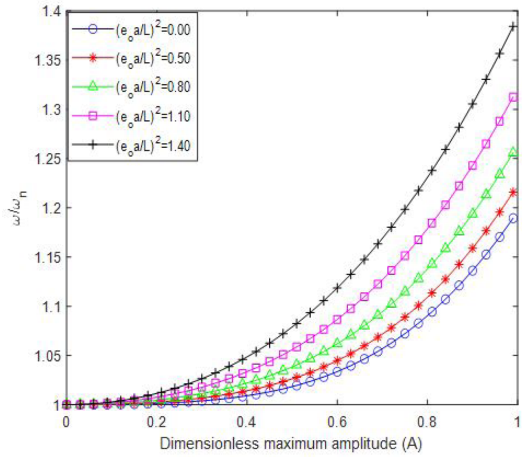

Figure 22: show effects of nonlocal parameter on nondimensional amplitude-frequency ratio on clamped-clamped supports

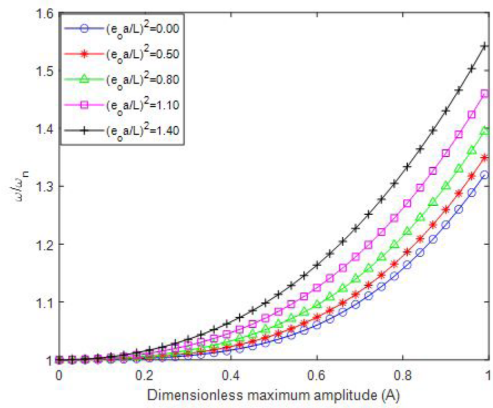

Figure 23: show effects of nonlocal parameter on nondimensional amplitude-frequency ratio on clamped-pinned supports

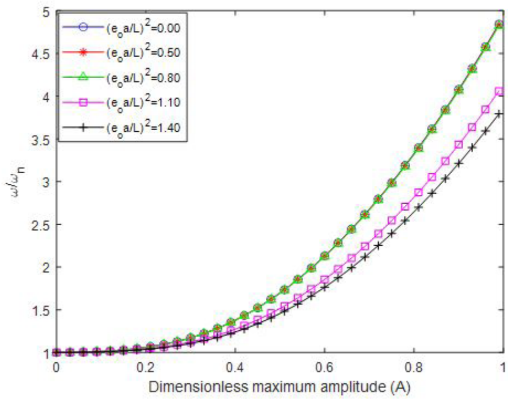

Figure 24: show effects of nonlocal parameter on nondimensional amplitude-frequency ratio on clamped-free supports

Figure 25, 26, 27 and 28 show influence of nonlocal parameter of different boundaries conditions on nondimensional amplitude-frequency ratio curve of vibration of single walled carbon nanotubes resting on elastic foundation with magnetic and thermal effects under the influence of Casimir force. Figure 21, 22 and 23 depict that as nonlocal parameter increases from zero to maximum, frequency-ratio increases as well. However, in such a manner the nonlocal parameter should be kept at minimum to stabilize stability analysis but for figure 24, nonlocal parameter should be kept at maximum.

Effect of Casimir Force on Frequency Ratio-Amplitude Curves for Different End Conditions

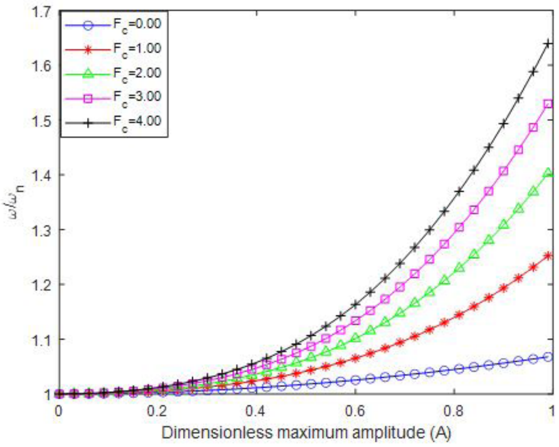

Figure 25: show effects of Casimir force on nondimensional amplitude-frequency ratio on pinned-pinned supports

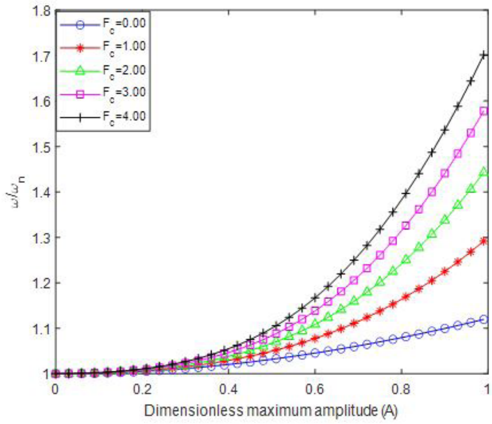

Figure 26: show effects of Casimir force on nondimensional amplitude-frequency ratio on clamped-clamped supports

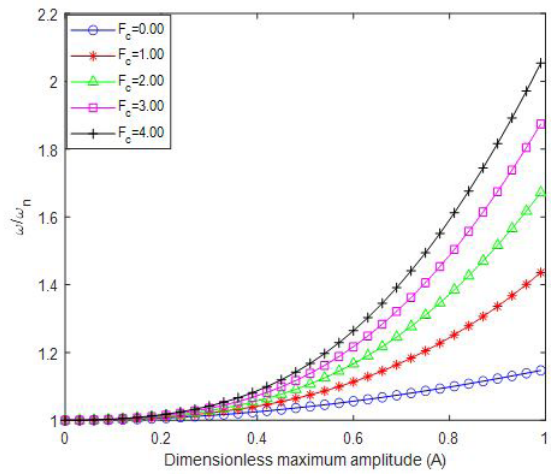

Figure 27: show effects of Casimir force on nondimensional amplitude-frequency ratio on clamped-pinned supports

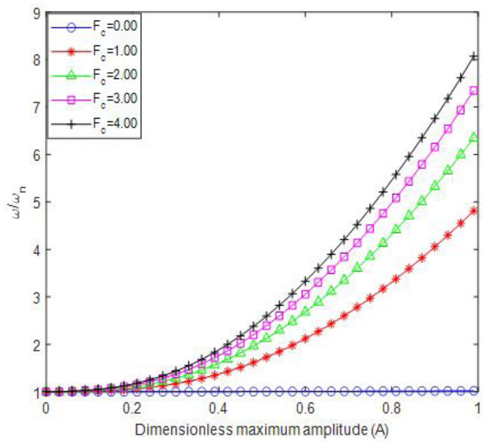

Figure 28: show effects of Casimir force on nondimensional amplitude-frequency ratio on clamped-free supports

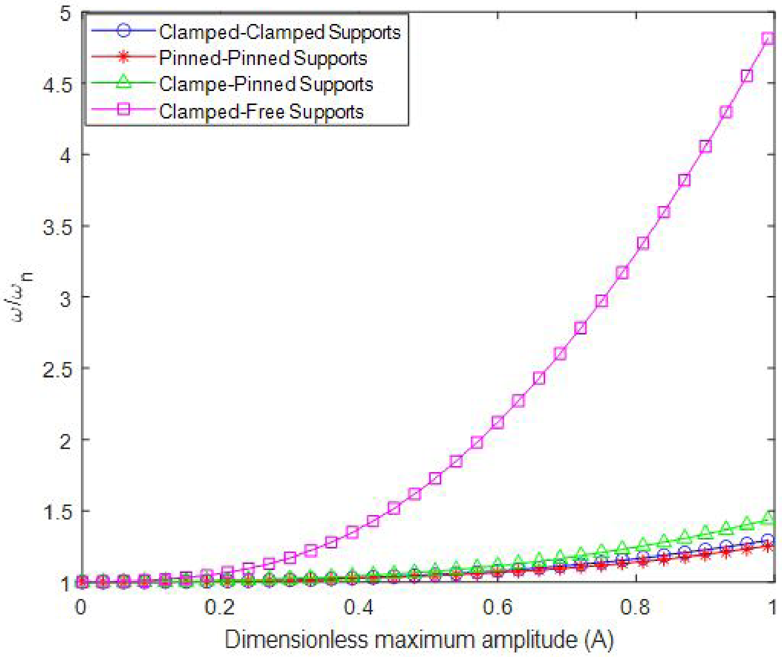

Figure 29: show effects of different boundary conditions on nondimensional amplitude-frequency ratio

Figure 29 show influence of different boundaries conditions on nondimensional amplitude-frequency ratio curve of vibration of single walled carbon nanotubes resting on elastic foundation with magnetic and thermal effects under the influence of Casimir force. Figure 29 depict that clamped-free supports has the highest frequency ratio. The pinned-pinned and clamped-clamped supports have lowest frequency ratio. Therefore, this reveal that in selecting elastic medium-type, pinned-pinned or clamped-clamped supports which exhibit best foundation-types with lowest frequency ratio can be used to control stability of any elastic medium under this study.

Effect of Casimir Force on Dynamic Response

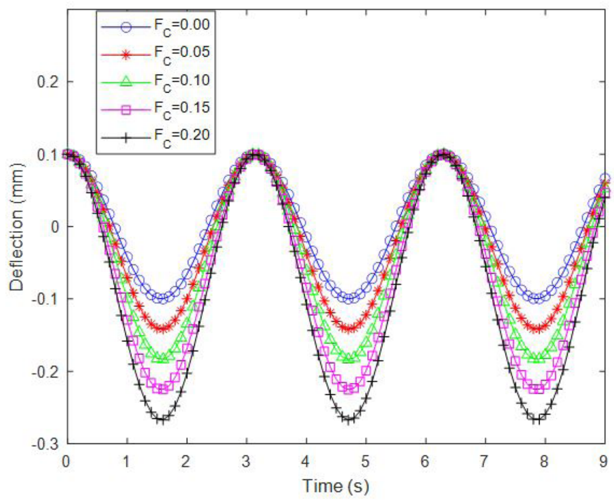

Figure 30: show effects of Casimir force on nondimensional Time-Deflection curve

Figure 30 show influence of Casimir force on time-deflection curve of vibration of single walled carbon nanotubes resting on elastic foundation with magnetic and thermal effects under the influence of Casimir force. The force concentrated at the compressive zone as way of improving serviceability, long term deflections and to provide support for stirrups throughout the beam when the system is subjected to serviceability limit state.

Conclusion

The dynamic response analysis of carbon nanotube has created noble attention globally owing to their excellent potential properties and application in fields of nanoscience, mechanical, electrical, materials science, reinforced composite structure and engineering construction since the evolution of the tiny materials decades ago. In this study, vibration of single walled carbon nanotube resting on elastic foundation with magnetic and thermal effects under the influence of Casimir force was studied. The governing nonlinear model derived using combined Eringen nonlocal theory, Euler-Bernoulli beam theory and Hamilton technique. The resulting partial differential equation of motions was converted to duffing equation using step-by-step Galerkin decomposition method. Consequently, the duffing equation is solve using analytical solution of homotopy perturbation method (HPM). The results obtained from the parametric study show how the magnetic term, thermal, Pasternak type medium, linear Winkler type, nonlinear Winkler type, nonlocal parameter, and Casimir force affect the nondimensional amplitude-frequency ratio and dynamic response of the system for all the boundary conditions considered. It is important to mention that an augmentation in Casimir force gives higher compression on time-deflection curve.

References

1. Andrzej Tylikowski (2006) Dynamic stability of carbon nanotubes, Mechanics and Mechanical Engineering, 10: 160–6.

2. Azrar A, Azrar L, ljinaidi AA (2014) Nonlinear Free Vibration of Single Walled Carbone Nanotubes Conveying Fluid, MATEC Web of Conferences 11: 02015-3.

3. Belhadj A Boukhalfa A, Belalia SA (2017) Free vibration modelling of single-walled carbon nanotubes using the differential quadrature method, Mathematical Modelling of Engineering Problems, 4: 33-37.

4. Hossain M and Lellep J (2021) Thermo mechanical vibration of single wall carbon nanotube partially embedded into soil medium, Agronomy Research,19: 777–87.

5. Jiayin Dai, Yongshou Liu, Guojun Tong (2020) Stability Analysis of a Periodic Fluid-Conveying Heterogeneous Nanotube System, Acta Mechanica Solida Sinica, 33: 756–69.

6. Lolov D, Lilkova-Markova S (2018) Dynamic Stability of Double-Walled Carbon Nanotubes, Journal of the Serbian Society for Computational Mechanics, 12: 1-8.

7. Mahdavi MH, Jiang LY, Sun X (2009) nonlinear vibration of a single-walled carbon nanotube CNT embedded in a polymer matrix aroused by van der Waals vdW forces, Journal of Applied Physics, 106: 114309-9.

8. Mir M Seyyed Fakhrabadia, Abbas Rastgoo, Mohammad Taghi Ahmadian (2015) Nonlinear Dynamic Analysis of Electrostatically Actuated Single-walled Carbon Nanotubes Using Nonlocal Elasticity, Latin American Journal of Solids and Structures, 12: 1224-40.

9. Mohammad Hosseini and Moslem Sadeghi-Goughari (2016) Vibration and Instability Analysis of Nanotubes Conveying Fluid Subjected to a Longitudinal Magnetic Field, Applied Mathematical Modelling, 40: 2560–76.

10. Mohsen Asghari and Jacob Rafati (2010) Variational Principles for Stability Analysis of Multi-Walled Carbon Nanotubes Based on A Nonlocal Elastic Shell Model, Proceedings of the ASME 10th Biennial Conference on Engineering Systems Design and Analysis 12-14.

11. Payam Soltani, Amir Kassaei, Mohammad M. Taherian and Anoushiravan Farshidianfar (2011) Vibration Analysis of Curved Single-Walled Carbon Nanotubes Embedded in An Elastic Medium Based on Nonlocal Elasticity, ICSV18, Rio de Janeiro, Brazil, 10-14.

12. Quan Wang, Yasuhide Shindo (2006) Nonlocal Continuum Models for Carbon Nanotubes Subjected to Static Loading, Journal of Mechanics of Materials and Structures, 1: 663-80.

13. Quan Wang, Ting Hu, Guanhua Chen and Qing Jiang (2005) Bending Instability Characteristics of Double-Walled Carbon Nanotubes, Physical Review B, 71: 045403-8.

14. Sang-Youl Lee, Ji-Gwang Hwang (2019) Finite Element Nonlinear Transient Modelling of Carbon Nanotubes Reinforced Fiber/Polymer Composite Spherical Shells with a Cutout, Nanotechnol Rev, 8: 444–51.

15. Shaba AI, Jiya M, Aiyesimi YM, Mohammed AA (2021) Vibration of Single – Walled Carbon Nanotube (SWCNT) on A Winkler Foundation with Magnetic Field Effect, Science World Journal, 16: 402-6.

16. Subrat Kumar Jena, S Chakraverty, Mohammad Malikan, Francesco Tornabene (2019) Stability Analysis of Single-Walled Carbon Nanotubes Embedded in Winkler Foundation Placed in a Thermal Environment Considering the Surface Effect Using a New Refined Beam Theory, Mechanics Based Design of Structures and Machines.

17. Tai-Ping Chang and Quey-Jen Yeh (2018) Innovative Material Technology: Chaotic Motion of Single-Walled Carbon Nanotube with Linear and Nonlinear Damping, Journal of Materials and Applications, 7: 96-110.

18. Venkatraman G, Suji D (2022) Solutions of Nonlinear Free Vibration of Single-Walled Carbon Nanotubes Conveying Fluid, Acta Physica Polonica A, 141: 218-25.

19. Yaxin Zhen (2016) Vibration and Instability Analysis of Double-Carbon Nanotubes System Conveying Fluid, J. Nanomech.

Micromech, 6: 04016008.

20. Ya-Xin Zhen (2016) Vibration and Instability Analysis of Fluid-Conveying Nanotubes Embedded in Visco-Elastic Medium with Consideration of Surface Effect, Mathematical Models in Engineering, 2: 108-113.

21. Yinusa AA, Sobamowo MG (2023) Nonlinear Thermal-Magneto-Mechanical Vibration Analysis of Single-Walled Embedded Branched Carbon Nanotubes Conveying Nanofluid. ASME Open Journal of Engineering, 2.

22. Yinusa AA, Sobamowo MG, Adelaja AO (2022) Thermal analysis of nanofluidic flow through multi-walled carbon nanotubes subjected to perfectly and imperfectly bonded wall conditions. Chemical Thermodynamics and Thermal Analysis, 5: 100028.

23. Yinusa AA, Sobamowo MG (2022) Mechanics of nonlinear internal flow induced vibration and stability analysis of a pre-tensioned SWCNT using classical DTM with CAT and SAT after treatment techniques. Forces in Mechanics, 7: 100083.

24. Yinusa AA, Sobamowo MG, Adelaja AO (2022) Flow induced bifurcation and phase-plane stability analysis of branched nanotubes resting on two parameter foundation in a magnetic environment. Partial Differential Equations in Applied Mathematics, 5: 100234.

25. Yinusa AA, Sobamowo MG, Adelaja AO (2020) Nonlinear vibration analysis of an embedded branched nanofluid-conveying carbon nanotube: Influences of downstream angle, temperature change and two-dimensional external magnetic field. Nano Material Science, 2: 323-32.

26. Yinusa AA, Sobamowo MG (2019) Analysis of Dynamic Behaviour of a Tensioned Carbon Nanotube in Thermal and Pressurized Environments. Karbala International Journal of Modern Science, 5: 1-11.